



N6718096

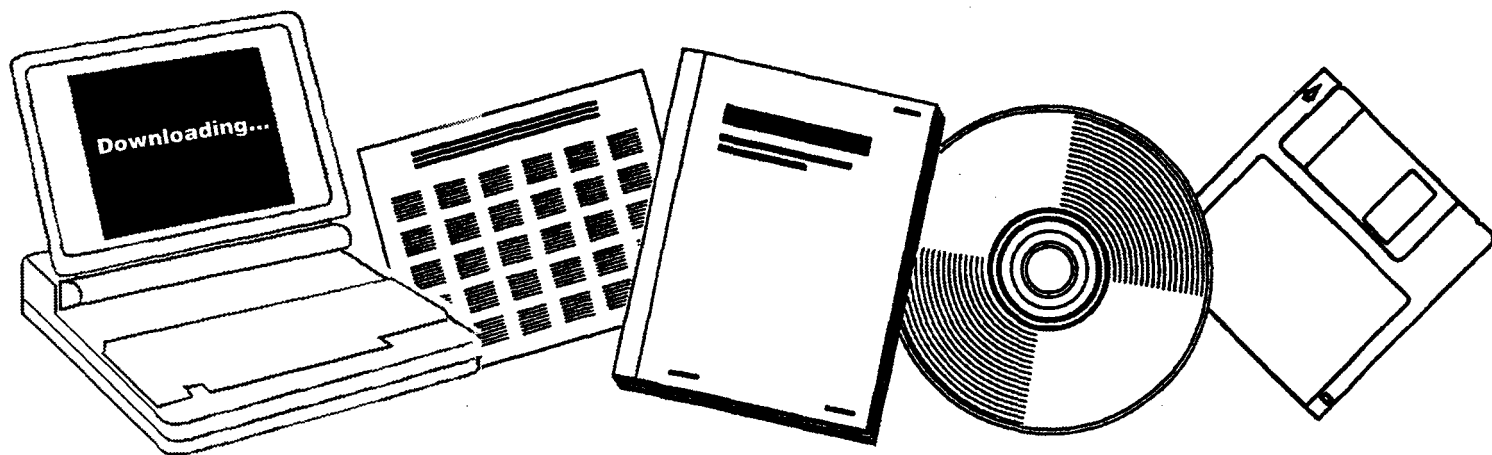
NTIS

One Source. One Search. One Solution.

FINAL REPORT ON NASA RESEARCH GRANT - STUDY OF HEAT TRANSFER THROUGH CONVECTION LAYERS

MECHANICAL ENGINEERING DEPARTMENT,
UNIVERSITY OF MINNESOTA

1966



U.S. Department of Commerce
National Technical Information Service

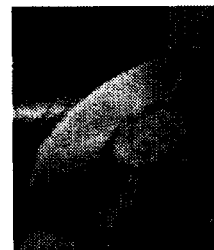
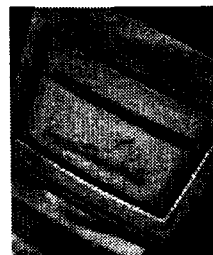
One Source. One Search. One Solution.

NTIS



Providing Permanent, Easy Access to U.S. Government Information

National Technical Information Service is the nation's largest repository and disseminator of government-initiated scientific, technical, engineering, and related business information. The NTIS collection includes almost 3,000,000 information products in a variety of formats: electronic download, online access, CD-ROM, magnetic tape, diskette, multimedia, microfiche and paper.



Search the NTIS Database from 1990 forward

NTIS has upgraded its bibliographic database system and has made all entries since 1990 searchable on **www.ntis.gov**. You now have access to information on more than 600,000 government research information products from this web site.

Link to Full Text Documents at Government Web Sites

Because many Government agencies have their most recent reports available on their own web site, we have added links directly to these reports. When available, you will see a link on the right side of the bibliographic screen.

Download Publications (1997 - Present)

NTIS can now provide the full text of reports as downloadable PDF files. This means that when an agency stops maintaining a report on the web, NTIS will offer a downloadable version. There is a nominal fee for each download for most publications.

For more information visit our website:

www.ntis.gov



U.S. DEPARTMENT OF COMMERCE
Technology Administration
National Technical Information Service
Springfield, VA 22161

N6718096

FINAL REPORT ON NASA RESEARCH GRANT

NsG 714/24 - 005 - 036

"Study of Heat Transfer Through Convection Layers"

by
R. J. Goldstein
and
T. Y. Chu

Mechanical Engineering Department
University of Minnesota
Minneapolis, Minnesota

1966

Reproduced from
best available copy

NOMENCLATURES

| | |
|----------------------------|--|
| D | Distance between plates or thickness of the fluid layer |
| Nu | Nusselt Number |
| n_o | The order of the marginally stable mode in the Malkus theory |
| Pr | Prandtl number |
| Ra | Rayleigh number |
| Ra_c | Critical Rayleigh number for the onset of convection |
| T | Absolute Temperature |
| T_1 | Temperature of the bottom plate |
| T_2 | Temperature of the top plate |
| TF | Center-line temperature or reference temperature $= (T_1 + T_2) / 2$ |
| T_z | Temperature at z above the bottom plate (or below the top plate) |
| z | Coordinate in the vertical direction above the bottom plate (or below the top plate) |
| θ | Dimensionless temperature difference $= 2(TF - T_z) / (T_1 - T_2)$ (Usually the absolute value is taken) |

INTRODUCTION

The purpose of the present investigation is to measure the heat transfer and mean temperature distribution with turbulent free convection in an air layer heated from below with constant non-slip boundaries. A Mach-Zehnder interferometer is used to measure the temperature field. The Mach-Zehnder interferometer has been used in various heat transfer studies (1, 2, 3) and it has shown to be capable of giving very accurate results. Since a light beam has no inertia, it is especially suitable for measuring rapidly varying turbulent flow. It is not possible to measure the mean temperature of turbulent convection in the usual sense of taking time average at particular position. Instead, with time exposure of the interferogram, the interferometer gives a combined space and time average of the temperature field. The light beam integrates the temperature fluctuations along its path, and the film integrates the varying interference pattern over the time of exposure. It is felt that, with a large enough system and a long enough time exposure, the interferograms do represent the true mean time temperature field. This essentially assumes that the time average at a fixed location is equal to the combined spatial-time average actually measured.

Aside from the investigation of turbulent free convection, some studies are also made concerning onset of flow at low Rayleigh numbers. The point of the onset of convection can be obtained by observing the change of the temperature field as the fluid layer is heated continuously.

CHAPTER I

EXPERIMENTAL APPARATUS AND PROCEDURE

Experimental Apparatus

The test section contains two aluminum plates. They are held horizontally and parallel to each other. The air gap between these plates is enclosed by insulation. Two glass windows permit the passage of a light beam through the air gap. Fig. 1 shows an overall schematic of the test section.

The aluminum plates are each $1\frac{1}{4}" \times 30" \times 20"$. They have grooves cut in the back for the circulation of water to maintain each plate at a constant temperature. The grooves are $\frac{1}{2}"$ wide and $\frac{3}{4}"$ deep. They are in the form of a flattened double helix so that the flow directions in two adjacent channels are always opposite to equalize the plate temperature. The back side of the plate is made of a quarter inch aluminum plate glued and screwed over the channel webs. The aluminum surfaces enclosing the fluid layer have been machined so that within the central span of the plate where the data are taken, the top plate is flat to within $\pm .001"$ and the bottom plate is flat to within $\pm 0.0005"$. Towards the corners of the plates they are still flat to within $0.003"$.

The plate temperatures are controlled by the two constant temperature water baths. Measurements with a thermocouple indicate no significant temperature variations around the plates. During the course of a seven junction copper-constantan thermocouple each plate measures the plate temperature.

The bottom plate is held horizontally. The top plate is supported by the bottom plate through bakelite corner supports with provision made for adjusting the vertical spacing. There is also a plexiglass spacer on each corner. The top plate is adjusted parallel to the bottom plate within 0.002". The fringes in the region close to the wall are not always clearly defined. Therefore, there is a small reference pin protruding from each plate to be used as reference points to determine the location of the wall.

The glass windows for the passage of the light beam are made of optical glass. They are each 6" in diameter and 1 mm in thickness. Each window is uniform in thickness to within $1/8$ wave length of the mercury light (5461 Å). The windows are first glued on bakelite frames and then fitted onto the openings on the insulation walls. The whole test section is insulated by styrofoam plates.

There are three steel balls attached to the backside of the bottom plate. They rest on triangular v-blocks fixed to the test section mount. The mount is made of angle iron. There are set screws on each leg of the mount and under the v-block assembly to hold the test plates horizontal. The mount is equipped with a hydraulic jack located directly under the test section. The hydraulic jack is used to lift the test section out of the light passage when adjustments are made on the interferometer. An overall view of the apparatus with the Mach-Zehnder interferometer is shown in Fig. 2.

Experimental Procedure

The initial alignment procedures of the Mach-Zehnder interferometer are standard. They are described in the report by Eckert, Drake, and Soehngen (1).

After the initial alignment of the interferometer, the test section is put into the test arm of the interferometer for fine alignment of the test section with the interferometer. A Nikon 35 mm camera with 10.5 cm focal length lens is used both to view and to record the interferograms. A minus 3 and a minus 1 auxiliary lens are used to focus the images on the camera screen. The camera is focused on the reference pins which are located in the focal plane of the interferometer. A white light is directed to the pins through the test section window while the camera is being focused.

The final alignment is to make the test plates horizontal and to adjust the relative position of the interferometer and the test section, so that the interferometric light beam is parallel to the central axis of the test section. First, the central axis of the test chamber is adjusted parallel to a vertical plane containing rays of the interferometric light beam. Two pins are taped at midpoint of each of the width sides of the bottom plate. The central axis is parallel to the vertical plane when the images of the two pins coincide on the camera screen. The plates are then aligned horizontally by a precision level. The light beam is made parallel to the plates through the adjustable springs which suspend the interferometer. One can judge whether the light beam is parallel to the plates by looking at the intersections of the vertical fringes with the plates

A vertical fringe on encountering a horizontal surface does not bend in either direction if the surface and the light are parallel. If the surface is turned slightly in either direction, the fringes are deflected on encountering the surface. Since the plates are parallel only within 0.002", only one plate (i. e., bottom one which is one from which temperature profiles are usually measured) can be aligned parallel to the light beam. The entire fine alignment procedure is repeated, if necessary, until the plates are properly aligned with the interferometer in every direction.

With all the alignment procedures completed, the heat transfer run begins. The plates are set at the room temperature for at least two hours before each run, to make sure that the air in the test section is at the room temperature. The straight fringes are aligned with a vertical plumb line. After the completion of the fine alignment, the test section is jacked out of the light passage. A picture of a precision scale held vertically is taken, with the scale placed at the focal plane of the interferometer. The picture of the scale is used to obtain the scale factor for evaluating the interferograms for each run.

The test section is then lowered and each plate is set at the desired temperature. In order to minimize the heat loss through the glass windows and reduce end effects, the temperature of the bottom plate and of the top plate are set equally above and below the room temperature. The inter-plate temperature difference varies from 4°C to 12°C . The plates are maintained at constant temperatures for one to two hours before the interferograms are taken. A Brown self-balancing potentiometer is used to measure

the EMF output of the thermopiles in the two plates.

Kodak Panatomic-x 35 mm film is used to record all interfero-grams. A piece of plastic vellum reduces the light intensity of the mercury lamp. The effect of the vellum is about the same as a 10% neutral density filter for the green light. The exposure time is 90 seconds with the shutter fully open. An additional 25% natural density filter is used for taking 5-minute time exposures. It is found, however, that 90 second time exposure is usually sufficient to obtain an average of the fluctuating fringe pattern of turbulent convection. For the runs on the onset of convection, 10 second exposures without the plastic vellum are used. Three to five interfero-grams are taken for each temperature difference. Two to five temperature differences are used for each run. Acufine fine grain developer is used to develop the films.

CHAPTER III RESULTS AND DISCUSSION

I. Turbulent Regime

A. Heat Transfer Results

The majority of the data are taken at two plate spacings.

The following table summarizes the range of the data taken:

| <u>Plate Spacings</u> | <u>Interplate Temperature</u> | <u>Rayleigh Number</u> |
|-----------------------|-------------------------------|--|
| 17.15 cm and 10.75 cm | 5.67°C to 11.70°C | 6.88×10^5 to 5.73×10^6 |

The heat transfer coefficients are calculated by using Fourier's law of conduction at the wall. The slope of the temperature distribution at the wall is obtained by a least square straight line fit of data points near the wall. The same computer program also calculates the Nusselt number and the Rayleigh number for each run.

Nusselt numbers and Rayleigh numbers are correlated in two ways. For high Rayleigh numbers ($Ra > 1.5 \times 10^6$), one-third power law fits the data well. The best fit is

$$Nu = 0.067 (Ra)^{1/3} \quad Ra > 1.5 \times 10^6 \quad (1)$$

The standard deviation of data points from equation (1) is 4.7%. The best fit through the whole range of the data gives

$$Nu = 0.1777 (Ra)^{0.2681} \quad (2)$$

** The standard deviation used here is a fractional deviation. It is the ratio of the standard deviation of the coefficient in the heat transfer correlation and the best value of the coefficient.

If one uses the usually assumed one-third power law over the whole range of Ra , the correlation is

$$Nu = 0.069 (Ra)^{1/3} \quad (3)$$

Equations (2) and (3) give results within 5% in the whole data range.

The heat transfer correlations are plotted in Fig. 3 and Fig 4. The standard deviation of the data points from equation (2) is 3.5% whereas for equation (3), it is 5.3%

The recent experiment by Globe and Dropkin (4), using water and silicone oil as working fluids, yields exactly the same results as equation (3) when the Pr of air is used in their correlation. In Silveston's summary (5) of all the available existing data for the heating from below problem, the Nusselt number is given as

$$Nu = 0.104 (Ra)^{0.305} (Pr)^{0.084} \quad (4)$$

Since the exponent is different from the present experiment, equation (4) is plotted together with the present result in Fig. 4 for comparison. They are in very good agreement.

B. Temperature Distribution in the Fluid Layer

Because of the restricted dimension of the field of view of the interferometer, only the lower part of the temperature field is evaluated with the present spacings. A typical interferogram is shown in Fig. 5. A typical temperature distribution in the form of θ versus z/D is plotted in Fig. 6. The profile has the general shape that one would expect. A steep gradient exists near the wall and decreases as one goes further into the fluid. Finally, the fluid appears to reach the center-line temperature.

From that point on, the mean temperature is almost constant until the vicinity of the upper plate. In other words, there exists a turbulent core in the fluid layer where the temperature gradient is nearly zero. An overshoot of the temperature profile outside the boundary as predicted by many numerical calculations (6) (7) (8) (9) (10) is not found in the present experiment.

The Malkus theory predicts the temperature distribution in the fluid layer to be

$$\bar{\theta} = \frac{1}{2\pi(n_0+1)} \cot \frac{\pi z}{D} \quad \left(\frac{z}{D} \gg \frac{1}{n_0} \right) \quad (5)$$

and

$$\theta = \frac{1}{2\pi^2(n_0+1)} \left(\frac{z}{D} \right)^{-1} \quad \left(\frac{1}{n_0} \gg \frac{z}{D} \gg \frac{1}{2\pi(n_0+1)} \right) \quad (6)$$

where (n_0+1) is simply the Nusselt number (13). In order to make comparison with the Malkus theory, the temperature distributions are plotted on log-log scales. If the Malkus theory is valid, there should be a portion of the curve that would fit to a straight line of slope minus one between the two assigned limits. The curve is shown in Fig. 7. The arrowheaded line and the two short bars indicate the limits between which the minus one power law should apply. The dashed line is the temperature distribution predicted by the Malkus theory, equation (6). The discrepancy between the theory and present experiment is large. However, it is possible to fit a small portion of the curve between the limits with a straight line of

slope minus one. This suggests that there might be a tentative agreement with the Malkus theory possibly off by a constant. But, this agreement is quite marginal. Since the curve shows a continuous change of slope, it is really possible to fit any straight line of any slope between $-1/2$ to -2 through a portion of the curve. But it is not possible at all to fit any part of the data to the $z^{-1/3}$ law proposed by Priestley.

Townsend (15) measured turbulent convection of air over a heated horizontal plate in 1957. Part of his experiment was for convection between parallel plates. Temperature distributions for three Rayleigh numbers, 0.85×10^5 , 3.77×10^5 , and 6.75×10^5 were measured. For the highest Rayleigh number, an overshoot of the temperature profile near the upper plate outside the boundary layer was found. Townsend attributed it to the onset of large circulations of dimensions similar to those of the whole apparatus. The main part of the paper concerned measurements of turbulent convection over a single heated horizontal surface. These data should resemble the convection for very high Rayleigh numbers. Townsend was able to find a universal temperature profile based on his dimensionless parameters θ_0 and Z_0 which were defined in his paper. The universal temperature profile is

$$\left(\frac{\ln(T_Z/TF)}{\theta} \right) \left(\frac{Z}{Z_0} \right) = 3.0 \quad (7)$$

His data agree with the Malkus theory except that the constant is 3.0 rather than 2.0 as required by the theory.

Some of the temperature distributions in the present experiment are put into the $\frac{\ln T_z / T_F}{\theta_0}$ and $\frac{Z}{Z_0}$ coordinates for comparison with Townsend's data, Fig. 9. The general trend is the same; however, the present data show a much faster drop of temperature outside of the boundary layer. Part of the discrepancy probably comes from Townsend's uncertainty about the ambient temperature. The outside air current may also have some effect on his open box apparatus.

II. The Onset of Convection

For gases the fringe shift and temperature follow almost exactly a straight line relation. Therefore, in the conduction regime where the temperature distribution is linear, the fringes are straight. When convection starts, the fringes start to bend. The fringes will bend more and more as the Rayleigh number increases. One can define the deviation of a fringe from a straight line at the wall as Δ . If one plots Δ vs. the Rayleigh number, the point where Δ becomes zero would be the point of the onset of convection. Since data are taken near the critical Rayleigh number, a least square straight line fit is used to extrapolate back to the critical Rayleigh number.

Two series of runs have been made to find the critical Rayleigh number. The two series of runs give results of $Ra_c = 1789$ and $Ra_c = 1777$. The result of one of the runs is shown in Fig. 8.

Taking an average of the two runs, the critical Rayleigh number is found to be 1783. The error is estimated to be ± 60 . This is in close agreement with the result of Thompson and Sogin. $Ra_c = 1793 \pm 80$ (16). Their work is the only accurate measurement using gases as working fluids.

CHAPTER IV

CONCLUDING REMARKS

From the present experiment the following conclusions can be drawn:

1. The critical Rayleigh number for the onset of convection in a horizontal air layer heated from below with rigid-rigid isothermal boundary conditions is experimentally found to be $Ra_c = 1783 \pm 60$. The result is in very good agreement with recently reported results. It is also in reasonable agreement with the theoretical value of 1708.

The heat transfer by free convection in a horizontal air layer for Rayleigh numbers between 6×10^5 and 6×10^6 can be correlated as

$$Nu = 0.1777 (Ra)^{0.268}$$

If one uses the usually assumed one-third power law over the whole range of Ra , the correlation is

$$Nu = 0.069 (Ra)^{1/3}$$

For high Rayleigh numbers ($Ra > 1.5 \times 10^6$), one-third power law fits the data well. The best fit is

$$Nu = 0.067 (Ra)^{1/3}$$

The above correlations are in good agreement with previous investigations using mainly high Prandtl number fluids.

3. The temperature distributions in the fluid layer have the general shape that one would expect, but the experimentally found temperature distributions do not show any close agreement with existing theories. They only show a marginal agreement with the Z^{-1} power law of the Malkus theory.

4. Although the contract has been officially ended, some more data are still being taken for high Rayleigh numbers. The few available heat transfer data points at Rayleigh numbers around 10^8 agree with equation (2) within approximately 8%. The agreement is good considering the extent of extrapolation.

BIBLIOGRAPHY

1. Eckert, E. R. G., R. M. Drake, and E. Soehngen, "Manufacture of a Zehnder-Mach Interferometer," Air Force Rep. 5721, ASTI N-34235 (1943).
2. Eckert, E. R. G. and E. Soehngen, "Studies on Heat Transfer in Laminar Free Convection with the Zehnder-Mach Interferometer," Air Force Rep. 5747, ASTI N-44580 (1948).
3. Eckert, E. R. G. and E. Soehngen, "Distribution of Heat Transfer Coefficients around Circular Cylinders in Crossflow at Reynolds Numbers from 20 to 500," Trans. ASME, 74, 343 (1952).
4. Globe, S. and D. Dropkin, "Natural Convection Heat Transfer in Liquid Confined by Two Horizontal Plates and Heated from Below," Trans. ASME, J. Heat Transfer, 81, 24 (1959).
5. O'Toole, J. L. and P. L. Silveston, "Correlation of Convective Heat Transfer in Confined Horizontal Layers," Chem. Eng. Progr. Symposium Series, 57, No. 32, 81 (1961).
6. Herring, J. R., "Investigation of Problems in Thermal Convection," J. Atmos. Sci., 20, 325 (1963).
7. Herring, J. R., "Investigation of Problems in Thermal Convection: Rigid Boundaries," J. Atmosph. Sci., 21, No. 3, 277 (1964).
8. Howard, L. N., "Heat Transport by Turbulent Convection," J. Fluid Mech., 17, 405 (1963).
9. Fromm, J. E., "Numerical Solutions of the Non-linear Equations for a Heated Fluid Layer," Phys. Fluids, 8, No. 10, 1757 (1965).
10. Deardorff, J. W., "A Pseudo-Three-Dimensional Numerical Study of Thermal Turbulence," J. Atmosph. Sci., 21, 419 (1964).
11. Malkus, W. V. R., "Discrete Transitions in Turbulent Convection," Proc. Roy. Soc. London, Series A, 225, 185 (1954).
12. Malkus, W. V. R., "The Heat Transfer and Spectrum of Thermal Turbulence," Proc. Roy. Soc. London, Series A, 225, 196 (1954).
13. Spiegel, E. A., "On the Malkus Theory of Turbulence," p. 181, Mecanique de la Turbulence, Edition du CNRS, Paris (1962).

14. Malkus, W. V. R., "Outline of a Theory of Turbulent Convection," Theory and Fundamental Research in Heat Transfer, Proc. of the Annual Meeting of the Amer. Soc. of Mech. Eng., New York, November, 1960, Ed. J. A. Clark, New York, Pergamon (1963).
15. Thomas, D. B. and Townsend, A. A., "Turbulent Convection over a Heated Horizontal Surface," J. Fluid Mech., 2, 473 (1957).
16. Thompson, H. A. and M. M. Sogin, "Experiments on the Onset of Thermal Convection in Horizontal Layers of Gases," J. Fluid Mech., 24, 451 (1966).

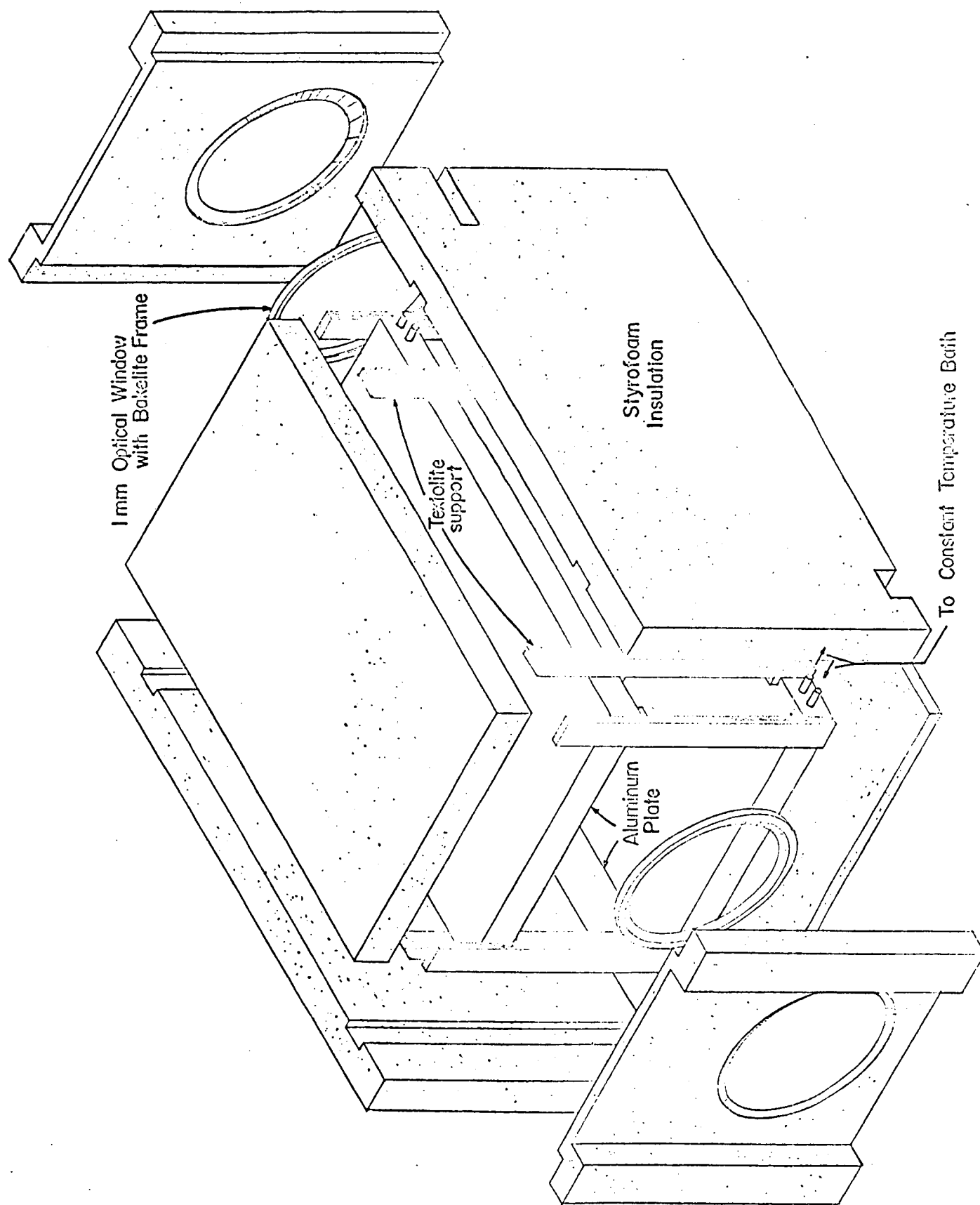


FIG. 1 AN OVERALL SCHEMATIC OF THE TEST SECTION

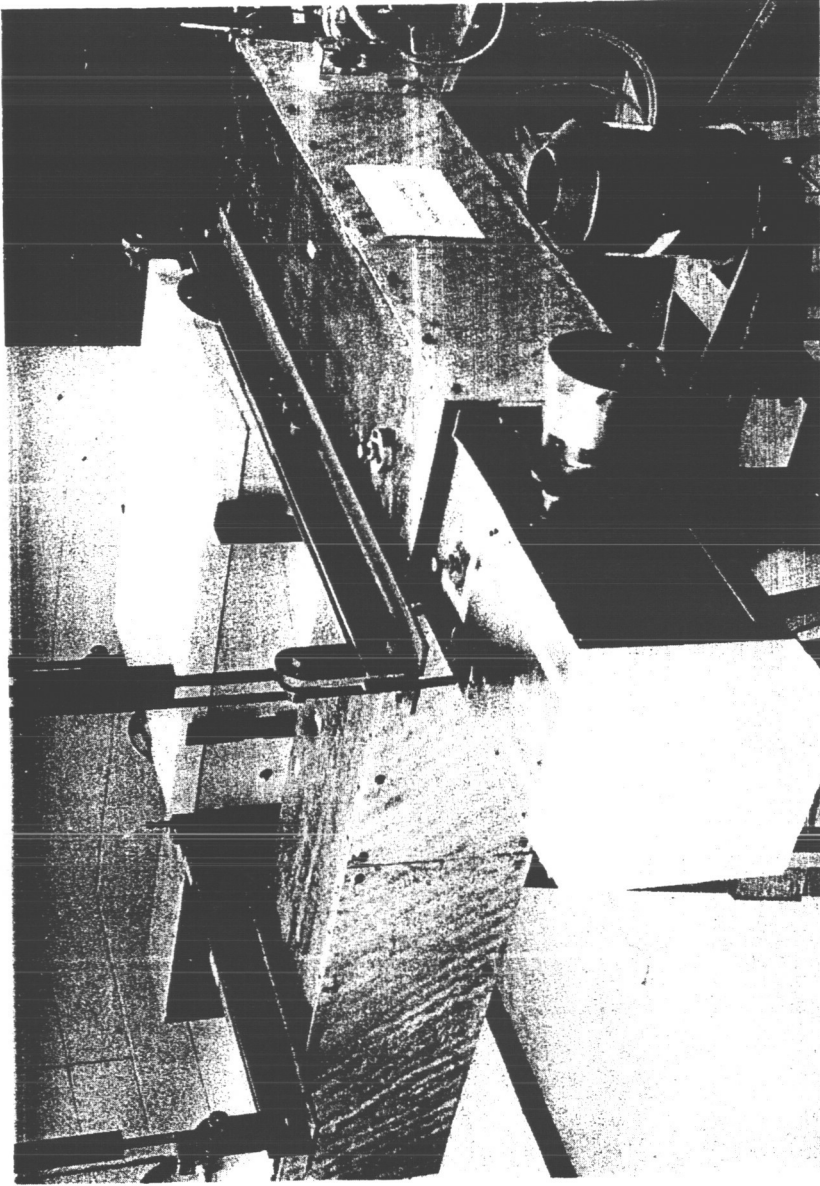


FIG. 2 THE TEST SECTION AND THE MACH-ZEHNDER INTERFEROMETER

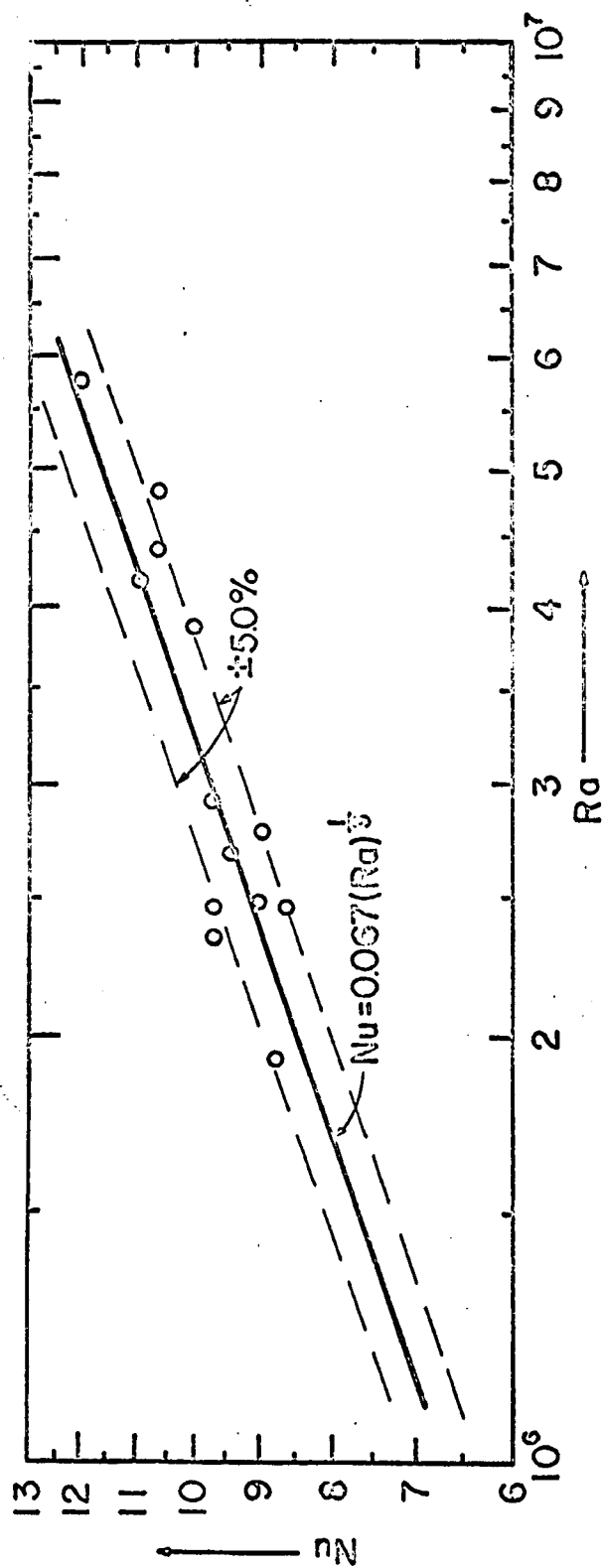


FIG. 3 FREE CONVECTION THROUGH A HORIZONTAL AIR LAYER

($Ra > 1.5 \times 10^6$)

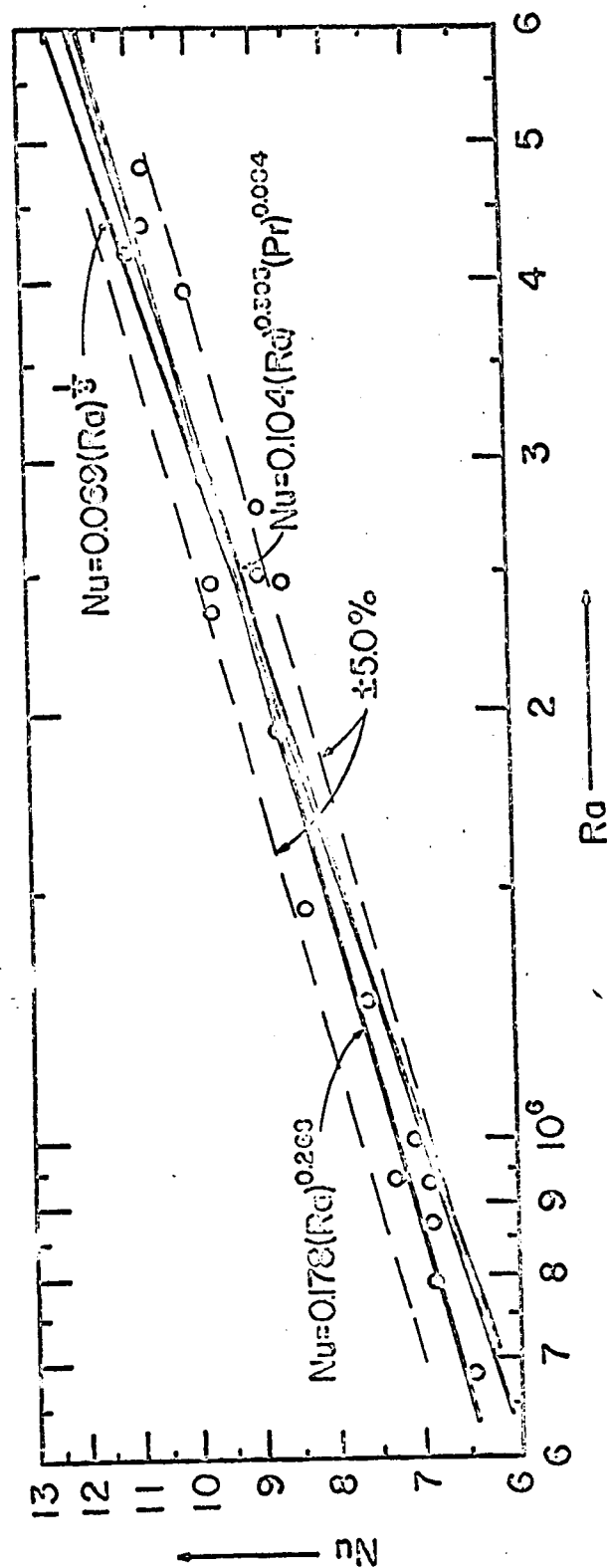


FIG. 4 FREE CONVECTION THROUGH A HORIZONTAL AIR LAYER
 $(6 \times 10^5 < Ra < 6 \times 10^6)$

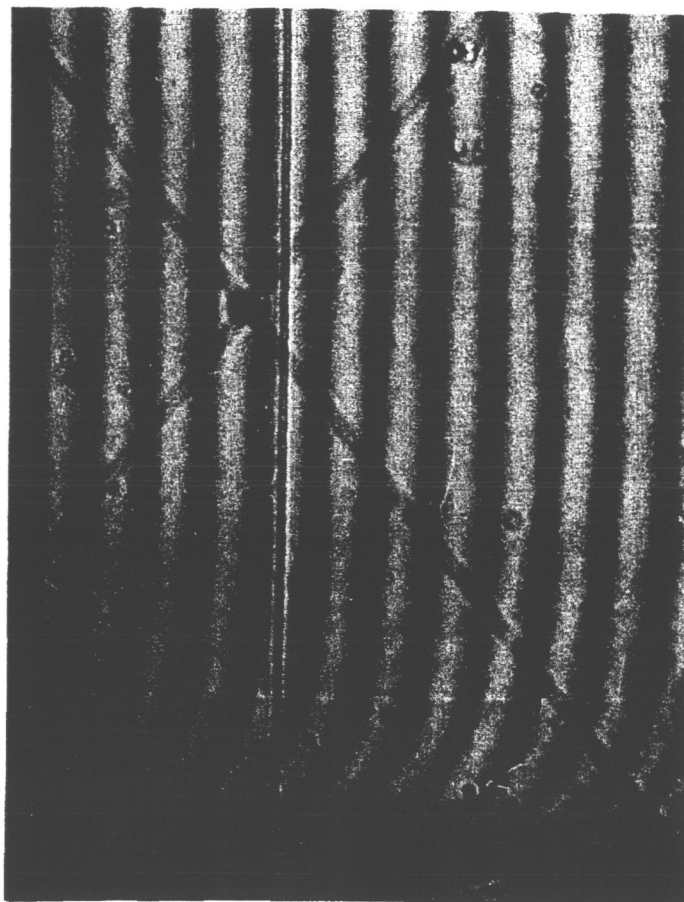


FIG. 5 TURBULENT FREE CONVECTION

INTERPLATE TEMPERATURE = 9.76°C

PLATE SPACING = 17.15 cm

RAYLEIGH NUMBER = 4.39×10^6

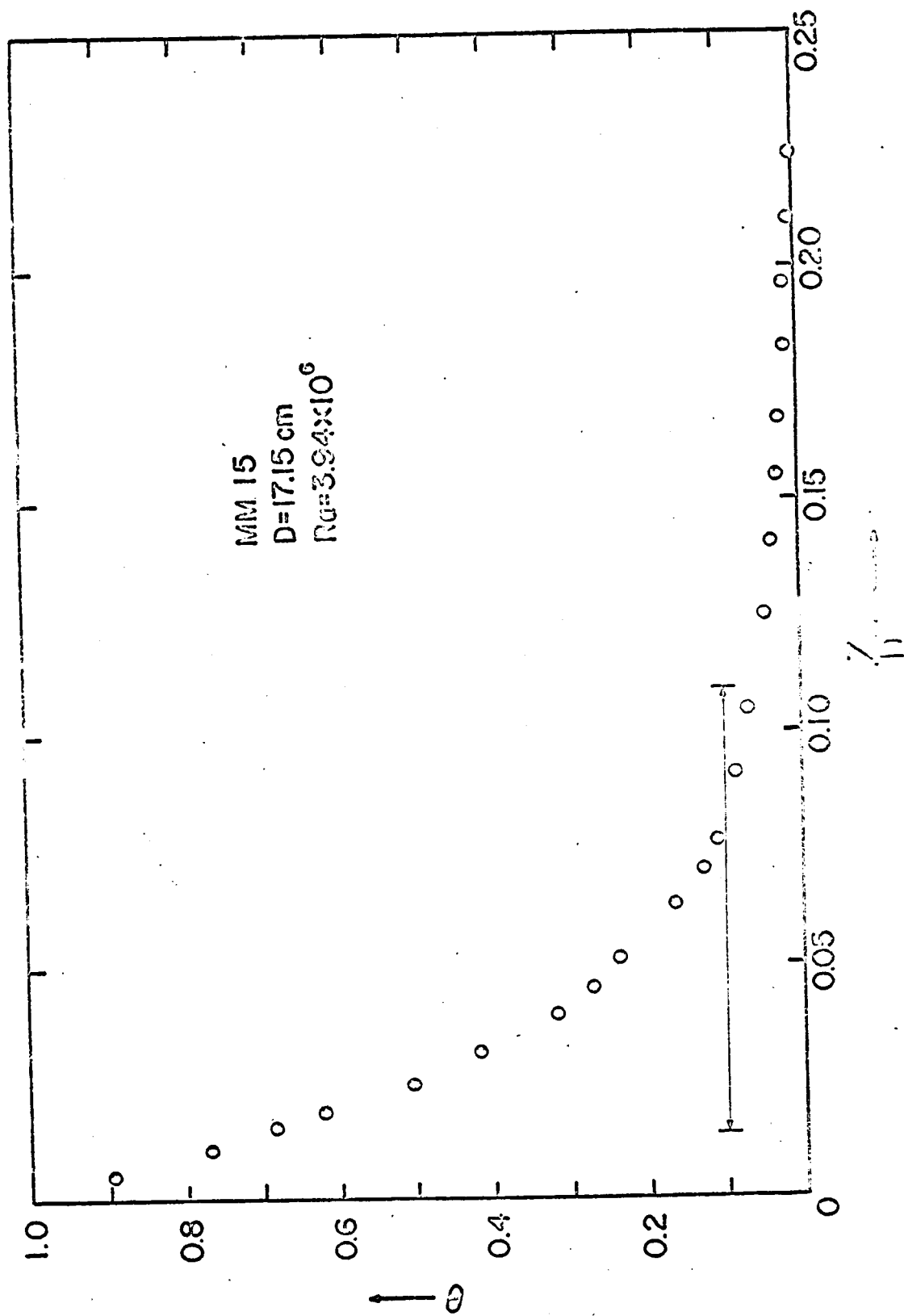


FIG 6. TEMPERATURE DISTRIBUTION IN A HORIZONTAL AIR LAYER (from bottom toward center)

The arrowheaded line indicates the range of application of Malkus' z^{-1} power law.

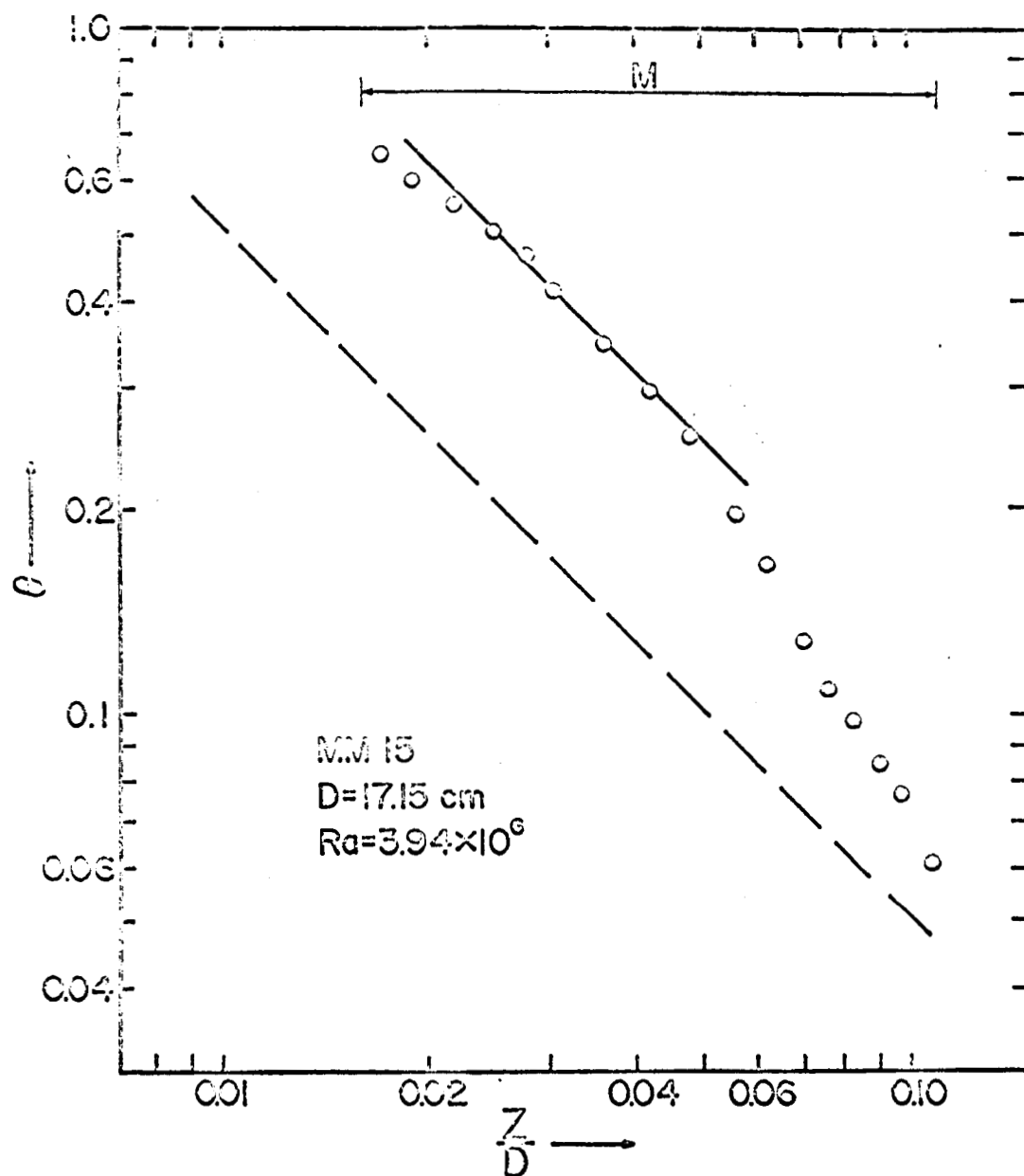


FIG 7. TEMPERATURE DISTRIBUTION IN A HORIZONTAL AIR LAYER (from bottom surface toward center)

The line marked M indicates the range of application of the z^{-1} power law. The dashed line is the theoretical temperature distribution from Malkus' Theory.

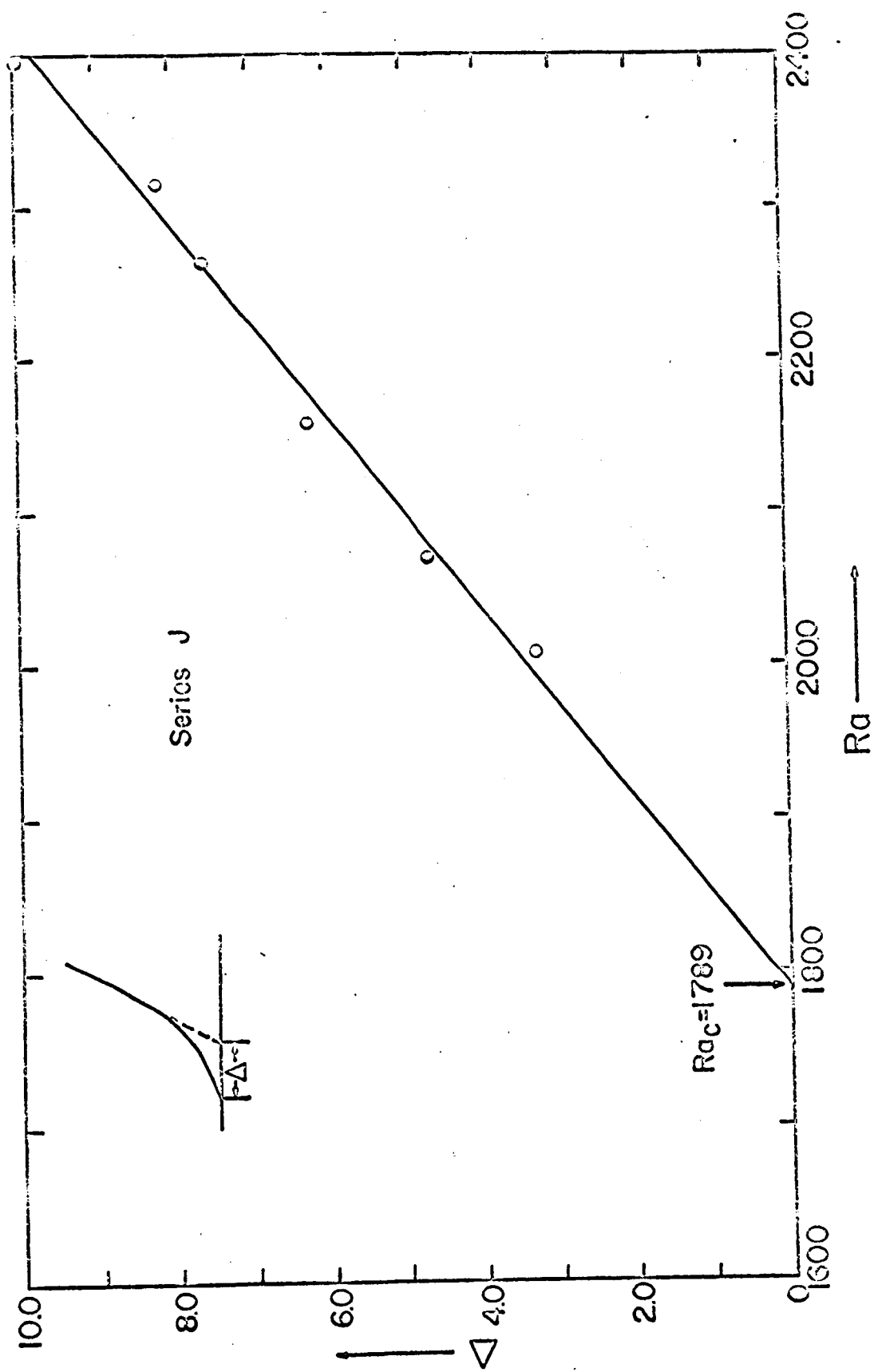


FIG. 8 EXTRAPOLATION FOR FINDING THE POINT OF THE ONSET OF CONVECTION

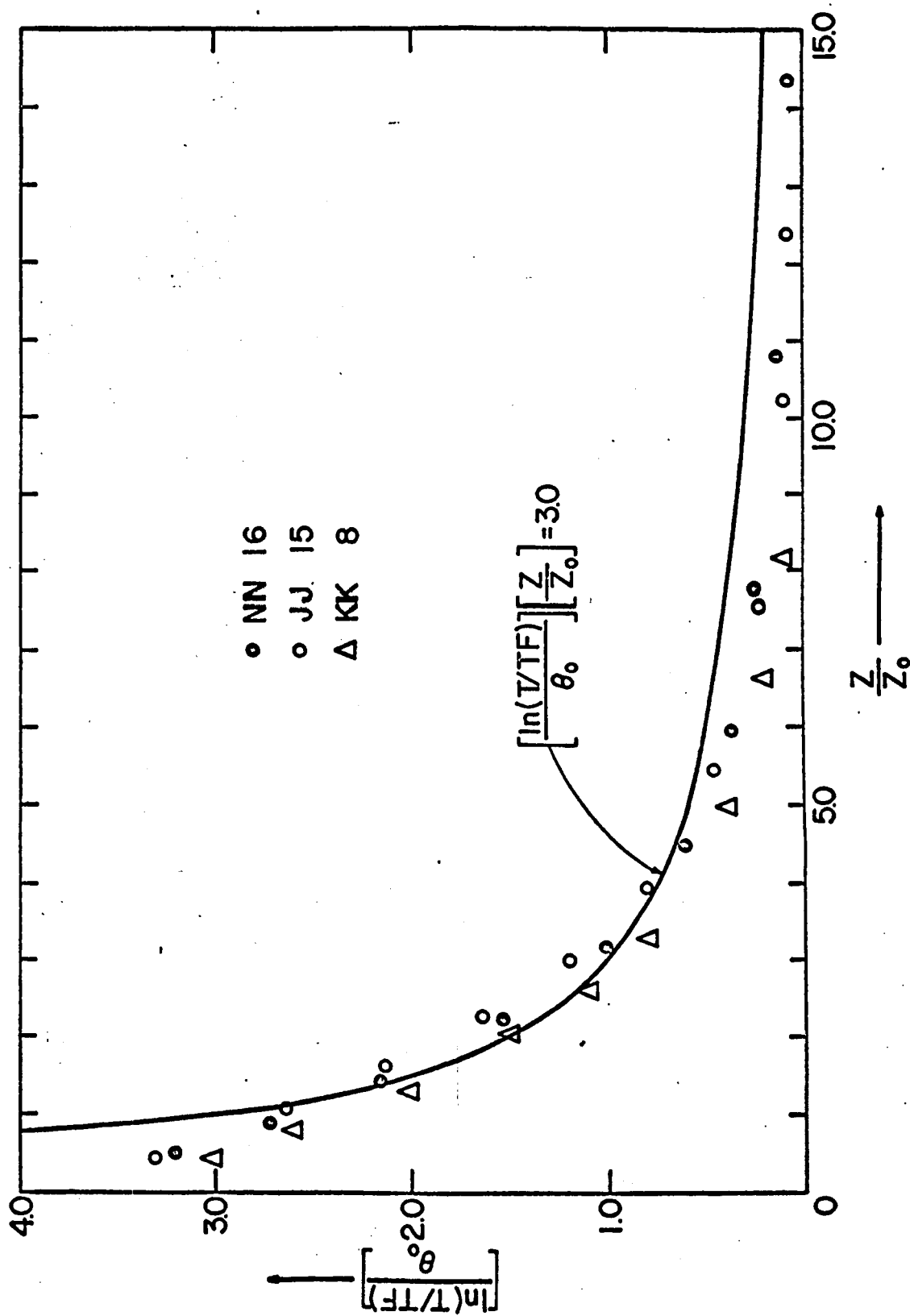


FIG. 9 TEMPERATURE DISTRIBUTION IN A HORIZONTAL AIR LAYER IN TOWNSEND'S COORDINATES